

4-16-80

2620 PI

NRL Report 8365

Transduction with PVF_2 in the Ocean Environment

YORAM BERLINSKY

*Underwater Sound Reference Detachment
P.O. Box 8337
Orlando, Florida 32856*

March 28, 1980



**NAVAL RESEARCH LABORATORY
Washington, D.C.**

Approved for public release; distribution unlimited

REPORT DOCUMENTATION PAGE		READ INSTRUCTIONS BEFORE COMPLETING FORM
1. REPORT NUMBER NRL Report 8365	2. GOVT ACCESSION NO.	3. RECIPIENT'S CATALOG NUMBER
4. TITLE (and Subtitle) TRANSDUCTION WITH PVF ₂ IN THE OCEAN ENVIRONMENT	5. TYPE OF REPORT & PERIOD COVERED Interim report on a continuing NRL problem	
	6. PERFORMING ORG. REPORT NUMBER	
7. AUTHOR(s) Yoram Berlinsky*	8. CONTRACT OR GRANT NUMBER(s) N00173-77-D-0007 and N00173-79-D-0004	
9. PERFORMING ORGANIZATION NAME AND ADDRESS Underwater Sound Reference Detachment Naval Research Laboratory P.O. Box 8337 Orlando, Florida 32856	10. PROGRAM ELEMENT, PROJECT, TASK AREA & WORK UNIT NUMBERS NRL Problems S02-38 (0582-0) and S02-51 (0593-0) (Continues)	
11. CONTROLLING OFFICE NAME AND ADDRESS	12. REPORT DATE March 28, 1980	
	13. NUMBER OF PAGES 44	
14. MONITORING AGENCY NAME & ADDRESS (if different from Controlling Office)	15. SECURITY CLASS. (of this report) UNCLASSIFIED	
	15a. DECLASSIFICATION/DOWNGRADING SCHEDULE	
16. DISTRIBUTION STATEMENT (of this Report) Approved for public release; distribution unlimited		
17. DISTRIBUTION STATEMENT (of the abstract entered in Block 20, if different from Report)		
18. SUPPLEMENTARY NOTES * The author is from the staff of the Israel Ministry of Defense Armament Development Authority on sabbatical leave to Oak Harbour Marine Associates, a contractor of the Underwater Sound Reference Detachment, Naval Research Laboratory		
19. KEY WORDS (Continue on reverse side if necessary and identify by block number) Piezoelectric polymers Polyvinylidene fluoride Piezoelectric constants		
20. ABSTRACT (Continue on reverse side if necessary and identify by block number) Experimental methods were utilized to establish the piezoelectric properties of PVF ₂ in the one-dimensional (33-mode) and hydrostatic mode of operation. The coupler reciprocity method has been used for characterizing the PVF ₂ as a hydrophone and as a transmitter. This method gives the free-field voltage sensitivity and hence g —the piezoelectric voltage coefficient. Through K_{33}^T the relative dielectric constant, d —the piezoelectric strain coefficient is obtained. Measurements in the one-dimensional configuration were taken at 100 and 1000 Hz in the stress range 0-100 MPa, and at four temperatures: 40, 25, 15, and 3.5°C. Measurements in hydrostatic configurations were taken at 1000 Hz and at 25°C. (Continues)		

DD FORM 1473
1 JAN 73EDITION OF 1 NOV 65 IS OBSOLETE
S/N 0102-014-6601

10. Program Element, Project, Task Area & Work Unit Numbers (Continued)

Program Element: 61153N-11 & 62711N
Projects: RR011-08-42 & ZF11-121-003

20. Abstract (Continued)

Samples prepared from the same sheet of PVF_2 exhibit variations in piezoelectric activity, which are presented and discussed.

A comparison method has been used to characterize the PVF_2 as a dynamic pressure sensor; d was measured as a function of peak one-dimensional stress in the range 0-80 MPa and at four temperatures: 40, 25, 15, and 4.5°C. The strain coefficient was also measured as a function of the rise time of the loading pulse at a temperature of 25°C. The experimental results are shown and discussed. Comparison with typical ceramics and quartz transducers shows improved behavior of PVF_2 over them.

This report also summarizes NRL-USRD's evaluation of the pre-POSFET samples (PVF_2 on sapphire) assembled at Stanford University. They were tested with the reciprocity coupler for their receiving and transmitting characteristics in the "unbacked" and "backed" configurations. The pre-POSFET samples have lower sensitivity compared with NRL-USRD samples. They exhibit low-frequency resonances of the sapphire substrate, due to flexural mode of vibration. These resonances are damped when the sapphire is cemented onto a rigid body.

CONTENTS

INTRODUCTION	1
GENERAL PROPERTIES OF PVF ₂	2
CALIBRATION WITH THE RECIPROCITY COUPLER	3
TEMPERATURE DEPENDENCE OF THE DIELECTRIC CONSTANT	4
PIEZOELECTRIC CONSTANTS— ONE-DIMENSIONAL CONFIGURATION	4
PIEZOELECTRIC VOLTAGE COEFFICIENT FOR PVF ₂ IN VARIOUS CONFIGURATIONS SUBJECTED TO HYDROSTATIC PRESSURE	9
RECEIVING RESPONSE AS A FUNCTION OF FREQUENCY	12
TRANSMITTING RESPONSE AS A FUNCTION OF FREQUENCY	12
EVALUATION OF THE PRE-POSFET PIEZOELECTRIC TRANSDUCER	14
Dimensions	15
Capacitance and Dissipation Factors	17
Receiving Response of the Pre-POSFET Configuration	17
<i>Sensitivity as a Function of Hydrostatic Pressure — Sample 5</i>	18
<i>Frequency Response — Sample 5</i>	19
<i>Frequency Response — Sample 6</i>	21
<i>Frequency Response of NRL-USRD Pre-POSFET Sample</i>	22
<i>Frequency Response of PZT-4 on Sapphire</i>	22
Transmitting Response of the Pre-POSFET Configuration	23
Discussion	24
HIGH AMPLITUDE DYNAMIC STRESS TRANSDUCER	25

CONTENTS (Continued)

SUMMARY	29
ACKNOWLEDGMENT	30
REFERENCES	30
APPENDIX — List of Samples	32

TRANSDUCTION WITH PVF₂ IN THE OCEAN ENVIRONMENT

INTRODUCTION

The piezoelectric effect has been known for many years [1]. It expresses a relation between mechanical properties—stress and strain, and electrical properties—electric field and polarization. Some materials show intrinsic piezoelectricity like quartz, tourmaline, and Rochelle salt. It has been found with the development of ceramics, that piezoelectric properties can be imparted to the material through a process called polarization: heating the sample and applying a high static electric field. The field causes the domains in the material to be oriented, thus resulting in a remanent polarization in the material. Barium titanate and lead zirconate titanate are well known examples of such materials. Most of the piezoelectric materials also have ferroelectric properties and lose their remanent polarization at elevated temperature or pressure.

Piezoelectricity has also been found in organic compounds like woods [2,3] and bones [4], because natural conditions of growth have given the microcrystals a preferred orientation. This effect, however, is very weak. Several synthetic polymers [5] exhibit intrinsic piezoelectricity although the piezoelectric constants are small.

In recent years, attention has been given to polymers that can be polarized [6]. The basic poling technique is to heat the material, apply as high a dc field as can be sustained and cool to room temperature with the field applied. Mechanical deformation usually improves the results. These materials initially have microcrystals that are randomly oriented; therefore, the net resultant polarization is zero. The poling process causes them to be oriented, as in the case of ceramics, resulting in measurable piezoelectricity. Copolymers, which are mixtures of two polymers, have also been studied in search of better performance and simpler producibility. Some of them are listed in Ref. 5.

From all the known piezopolymers, the most promising is polyvinylidene fluoride (PVF₂ or PVDF), which exhibits the highest strain and voltage piezoelectric constants. The piezoelectric properties of PVF₂ depend on the poling process. A typical polarization cycle consists of heating to about 120°C, applying tension that causes elongation of 400-500% (usually in one direction), applying high electric field (of the order of 800 kV/cm), and cooling to room temperature. This cycle lasts for about half an hour. The mechanism of piezoelectricity induced in PVF₂ is not yet fully understood, although various theoretical approaches and supporting experimental data have been presented.

The basic mechanism involved bulk phenomena, especially orientation of dipoles in the crystalline phase of the PVF₂ [6-8]. Broadhurst [9] indicates that the largest contribution to the activity of PVF₂ arises from bulk dimensional changes rather than from changes in molecular dipole moments. Murayama [10] says that piezoelectricity

originates from the strain and may be characterized by the length-expansion constant d_{31} . Another mechanism proposed is the migration of ionic impurities [11].

Sussner [12] reviews some of the proposed mechanisms and the experimental data, concluding that the polarization induced in PVF₂ originates at the positive metal electrode and is inhomogeneous across the volume of the sample. Therefore, neither a bulk conduction nor a dipolar alignment in the crystalline phase is the basic mechanism for the strong polarization of PVF₂, and another mechanism like the injection of charges from the electrodes should be taken into account.

The controversial approaches in explaining the origin of the piezoelectricity of PVF₂ did not prevent researchers from proposing and testing many devices in various fields of technology. Some air acoustic devices like headphones, speakers, and microphones are already commercially used. Hydrophones for underwater acoustics have been described [13,14]. Application of PVF₂ films to ultrasonic transducers for the generation and detection of ultrasounds in solids, liquids, and air are reported by Chubachi [15]. PVF₂ has been proposed for detecting structural defects in aircraft [16]. Devices for high-frequency medical imaging are described in [17-19]. High amplitude loading of PVF₂ for impact pressure measurement and for fuze applications are described in [20,21]. Some other applications utilize the pyroelectric effect of the polymer.

PVF₂ offers several potential applications in underwater acoustics. Some of these applications are:

- Wide-band low-noise hydrophone
- Shock sensor
- High-frequency transducer array (projector or receiver).

The piezoelectric polymers have been investigated to some extent, especially in the hydrophone mode of operation. Before they can be accepted and used in underwater acoustics, a material characterization of the polymer should be performed: the piezoelectric and dielectric properties as function of temperature, frequency, and pressure. These properties should be measured using calibration methods that imitate real operating conditions. This report summarizes the results obtained for PVF₂ at NRL-USRD.

GENERAL PROPERTIES OF PVF₂

PVF₂ has a density of 1.78×10^3 kg/m³ and longitudinal wave velocity of 2.15×10^3 m/s (acoustic impedance of 3.83×10^6 kg/m²s) [22]. It has a tensile strength of 25 to 30×10^7 N/m², tensile modulus of 200 to 250×10^7 N/m² (in the machine direction of the film), volume resistivity of 8 to 10×10^{12} Ωm, breakdown strength of 15 to 20×10^7 V(dc)/m, relative dielectric constant (1 kHz) of 12-13 and dissipation factor (1 kHz) of 0.02 - 0.03 [10].

PVF₂ is a flexible and compliant material that is easily attached to unusual surfaces. It can be rolled and unrolled; it can be produced in large sheets relative to ceramic pieces and in a wide range of thicknesses. It is chemically stable and unaffected by various

solvents. It is lightweight and seems to be highly shock-resistant. Its low acoustic impedance enables a good match to water and body tissues, so no matching network is needed.

Samples described in this report are cut from a 27- μm PVF₂ film, made by the Kureha Chemical Industry Co., Japan. The film is obtained in stretched, poled, and electroded form.

CALIBRATION WITH THE RECIPROCITY COUPLER

A convenient and powerful method for calibration in the hydrophone mode, or for determining the piezoelectric constants, is the coupler reciprocity method. The idea is to use a small chamber filled with fluid that acoustically couples three transducers. One of them is the hydrophone to be calibrated, and at least one of the others is reciprocal. A detailed description of reciprocity calibration can be found in [23,24]. A cross section of a coupler is shown in Fig. 1.

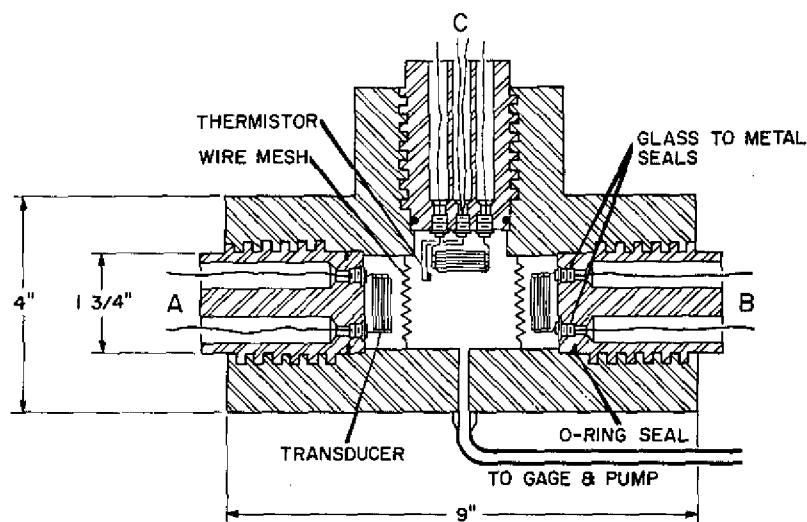


Fig. 1 — Cross section of reciprocity coupler calibrator

The coupler has very rigid boundaries and can withstand hydrostatic pressure up to 100 MPa. It is also temperature controlled. The fluid in the coupler is castor oil, whose compressibility as a function of pressure and temperature is known. In this type of calibration, an incremental periodical sound pressure is superimposed on the hydrostatic pressure. The calibration gives the free-field voltage sensitivity. If the stress applied on the sample is one dimensional, the piezoelectric voltage coefficient g_{33} is computed. It indicates the output voltage in the 3-axis produced by the stress in the 3-axis. Through K_{33}^T (the relative dielectric constant) in the 3-axis, the piezoelectric strain coefficient d_{33}

is computed. It indicates the polarization in the 3-axis produced by the stress in the 3-axis.

TEMPERATURE DEPENDENCE OF THE DIELECTRIC CONSTANT

The capacitance C of a sheet of PVF₂ having area A and thickness ℓ is measured at 1 kHz and, from this, the K_{33}^T is calculated:

$$K_{33}^T = \frac{C \cdot \ell}{\epsilon_0 A} \quad (1)$$

The sample consists of a square piece of PVF₂, 27 μm in thickness and $1.3225 \times 10^{-4} \text{ m}^2$ in area, cemented onto an aluminum substrate with conductive silver-filled epoxy. The sample is put in a temperature-controlled medium of polyalkylene glycol (PAG) and the temperature is varied from 0 to 45°C.

Results for the K_{33}^T show a linear dependence with temperature of the form:

$$K_{33}^T = 12.29 + 0.062T, 0^\circ\text{C} \leq T \leq 45^\circ\text{C}. \quad (2)$$

This result is in good agreement with the value reported in [10] for room temperature. The K_{33}^T is directly dependent on the film thickness, and uncertainty in the film thickness can cause variations in the measured value of K_{33}^T .

PIEZOELECTRIC CONSTANTS—ONE-DIMENSIONAL CONFIGURATION

A hydrophone in the reciprocity chamber is coupled to the acoustic source through a liquid and is therefore loaded by three-dimensional stress (a hydrostatic pressure and the sound pressure). In order to apply a one-dimensional loading on the PVF₂, the arrangement shown in Fig. 2 has been used. This configuration gives effective "33-mode" values of the piezoelectric constants that are the practical values to be used in transducer design. Effective "33-mode" values rather than actual values are obtained with the arrangement of Fig. 2, since the stainless steel endcaps clamp the lateral motion of the polymer, thereby reducing the measured value. The PVF₂ ($1.01 \times 10^{-4} \text{ m}^2$ in area) is cemented to the stainless steel electrodes with conductive silver-filled epoxy. This is identified as sample 1. The Appendix gives quick reference to all samples.

The one-dimensional static stress has been varied from atmospheric to 100 MPa. Measurements of the piezoelectric constants were made at 100 and 1000 Hz and at 40, 25, 15, and 3.5°C. The dielectric constant is measured (through the capacitance) at 1000 Hz, and it is assumed that the value at 100 Hz is practically the same.

The results are plotted in Figs. 3 to 6.

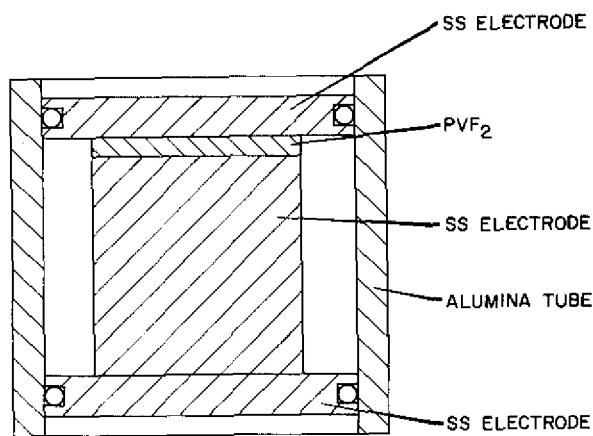


Fig. 2 - Configuration for obtaining one-dimensional stress

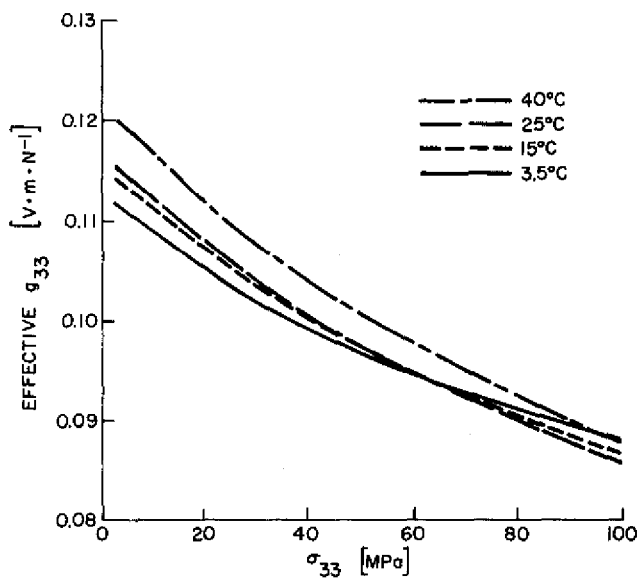


Fig. 3 - Effective piezoelectric voltage coefficient as a function of one-dimensional static stress at 1000 Hz

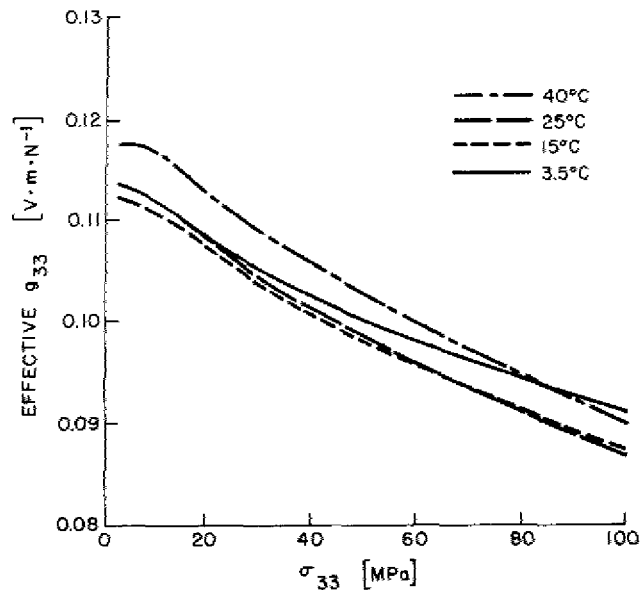


Fig. 4 — Effective piezoelectric voltage coefficient as a function of one-dimensional static stress at 100 Hz

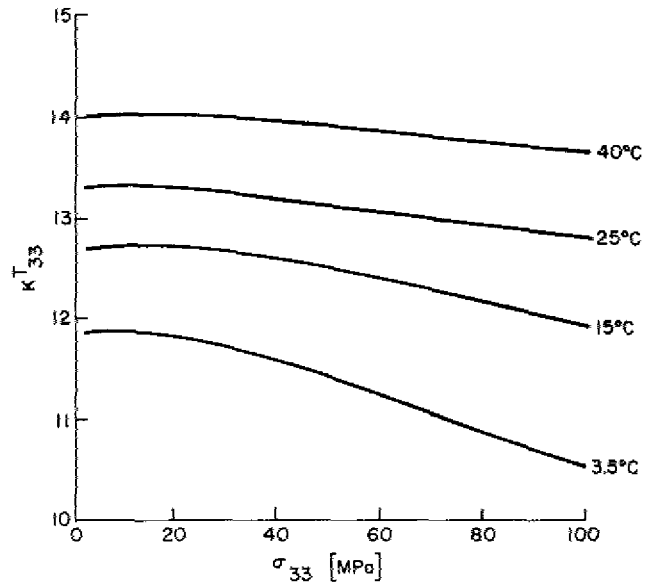


Fig. 5 — Relative dielectric constant as a function of one-dimensional static stress at 1000 Hz

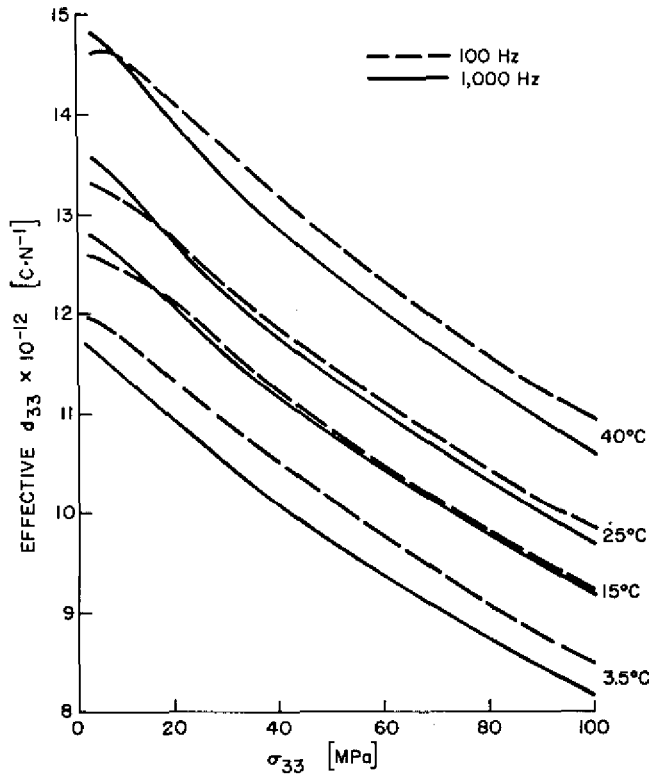


Fig. 6 — Effective piezoelectric strain coefficient as a function of one-dimensional static stress at 100 and 1000 Hz

Figure 3 shows the results for effective g_{33} measured at 1000 Hz as a function of one-dimensional static stress.

Figure 4 shows the results for effective g_{33} measured at 100 Hz as a function of one-dimensional stress. Notice that the deviation due to temperature from an average curve is $\pm 4\%$ ($\pm 0.3 \text{ dB}$) over the temperature range. The difference between results at 1000 and 100 Hz for a given temperature is less than $\pm 1.5\%$ ($\pm 0.1 \text{ dB}$).

Figure 5 shows K_{33}^T as a function of one-dimensional stress. The change of K_{33}^T with stress for a given temperature is relatively small: $\sim 10\%$ (0.8 dB) at 3.5°C and smaller for elevated temperatures. Results presented here for atmospheric pressure are about 5% higher than expected according to Eq. (2). It is believed that variation in the film thickness is the reason for these results.

Figure 6 shows effective d_{33} as a function of one-dimensional stress. The change with stress is mainly due to the change of g_{33} , and the change with temperature is mainly

due to the change of K_{33}^T . In all cases, neither g_{33} nor K_{33}^T has a hysteresis effect with stress; hence, d_{33} does not have it either.

Figure 7 compares normalized curves of effective g_{33} , K_{33}^T , and d_{33} of PVF_2 with those of a typical ceramic—PZT-4. The numbers in brackets are initial values to which these curves are normalized. The piezoelectric and dielectric constants of ceramics have a strong hysteresis effect (not shown in this figure) with stress [25] while PVF_2 does not. Therefore, PVF_2 has this basic advantage over them.

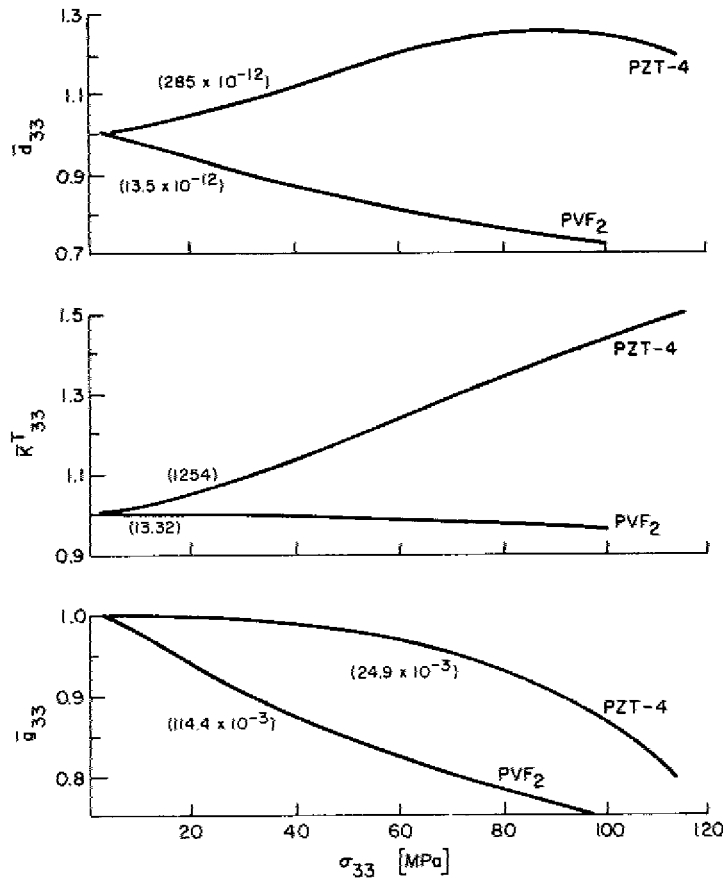


Fig. 7 — Normalized effective g_{33} , K_{33}^T , and d_{33} curves for PVF_2 and PZT-4. The bar over the constants signifies a normalized value.

Two additional samples have been tested in the same configuration. The results for effective g_{33} as a function of one-dimensional stress for 1000 Hz and 25°C are plotted in Fig. 8, together with that of sample 1 for the same conditions. A comparison between the three samples shows variations in effective g_{33} values of the order of 10%. The K_{33}^T has the

same value in each of the three cases (within $\pm 0.8\%$); therefore, the effective d_{33} has the same variations as the effective g_{33} between samples.

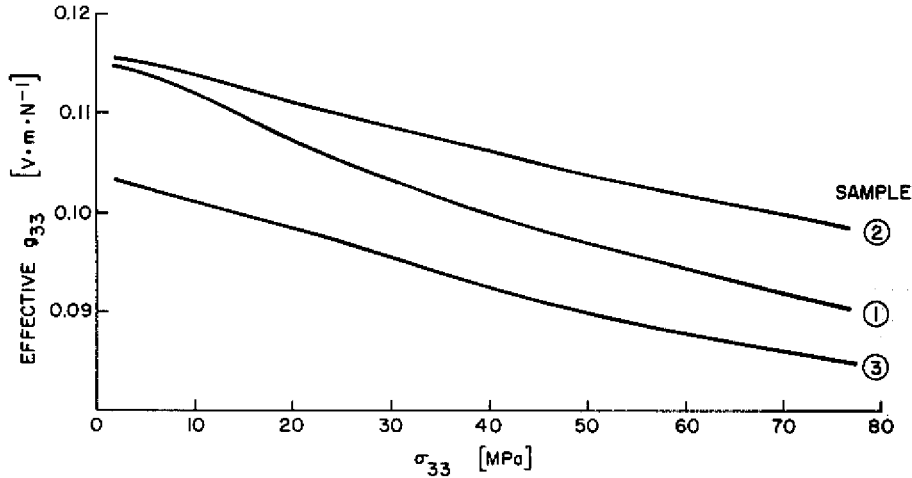


Fig. 8 — Effective piezoelectric voltage coefficient of three samples as a function of one-dimensional static stress at 1000 Hz and 25°C

The three samples were cut from the same sheet of PVF₂. The variation in thickness causes variation in the poling field; hence, the polarization across the film is inhomogeneous and is the reason for the difference in the effective g_{33} .

PIEZOELECTRIC VOLTAGE COEFFICIENT FOR PVF₂ IN VARIOUS CONFIGURATIONS SUBJECTED TO HYDROSTATIC PRESSURE

This section describes the experimental results obtained for the g_{33} of PVF₂ when the film is in direct contact with the fluid. Data have been taken using the coupler reciprocity method at 25°C and 1000 Hz.

Four configurations have been investigated. They are described in Fig. 9. In the first, the PVF₂ is clamped on both sides with stainless-steel electrodes (Fig. 9a). The samples are those described in the previous section for the one-dimensional case (Fig. 2) but with the alumina tube removed.

The second configuration is described in Fig. 9b. A circular piece of PVF₂ ($A \approx 3.88 \times 10^{-4} \text{ m}^2$) is cemented with conductive silver-filled epoxy onto a stainless-steel disc having the same area. Wire attachment to the top electrode is made using conductive gold-filled epoxy.

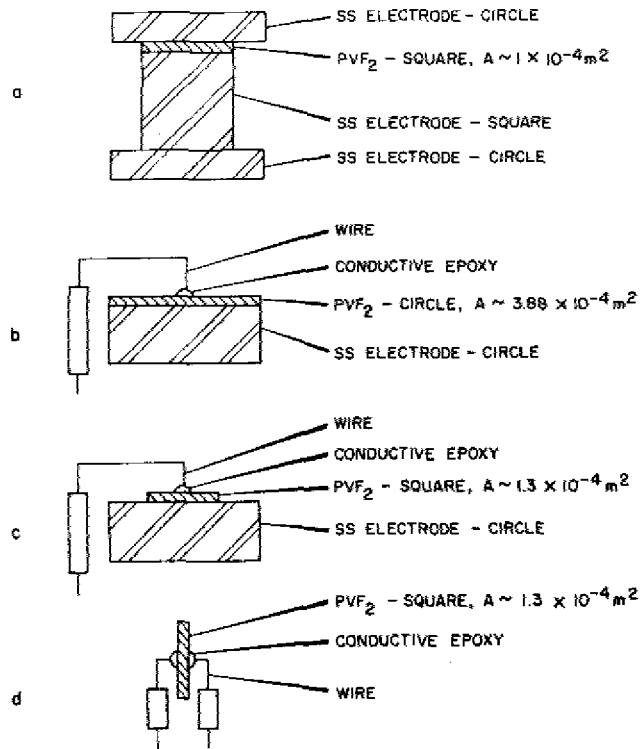


Fig. 9 — Four configurations for hydrostatic loading

The third configuration, shown in Fig. 9c, is basically the same except the PVF₂ is square and has an area of about $1.3 \times 10^{-4} \text{ m}^2$.

In the fourth configuration the PVF₂, square and having area of about $1.3 \times 10^{-4} \text{ m}^2$, is freely suspended in the castor oil (no backing). The pressure applied is completely hydrostatic. Wire contacts are made with conductive gold-filled epoxy (see Fig. 9d).

Two samples have been tested in the first configuration. They are marked a-2 and a-3 corresponding to the samples 2 and 3 mentioned in the previous section. A plot of g (the hydrostatic piezoelectric voltage coefficient) as a function of the hydrostatic pressure is presented in Fig. 10 (the two solid lines in the upper part marked a-2 and a-3). The g values obtained using the configuration shown in Fig. 9a (curves a-2 and a-3) and those obtained using the one-dimensional configuration (curves 2 and 3 of Fig. 8) are nearly the same as a function of pressure. This shows that there is no additional contribution of the stress component acting in the membrane direction, which is the direction of the plane of the film.

Two samples have been tested in the second configuration. The results obtained for g are plotted in Fig. 10—the two dashed lines marked b-1 and b-2.

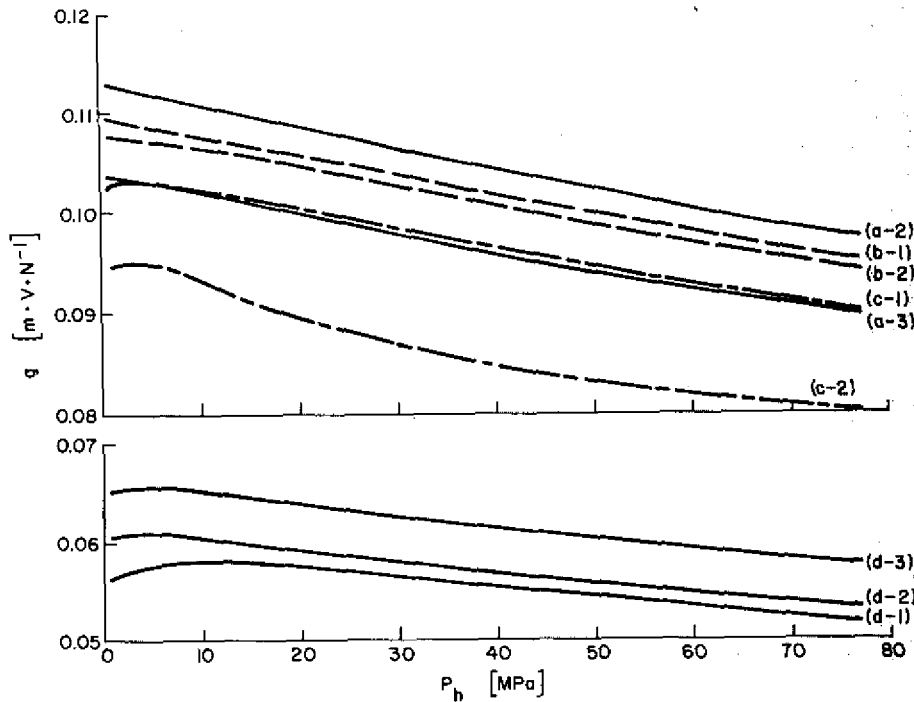


Fig. 10 -- Piezoelectric voltage coefficient of PVF_2 in four configurations as a function of hydrostatic pressure at 1000 Hz and 25 C

Two samples have been tested in the third configuration. The results for g are shown in Fig. 10—the two dash-dot lines marked c-1 and c-2. Curve c-1 is actually an average curve for two tests conducted on the same sample. The difference between the two tests was less than 0.5% above 4 MPa and about 2% at 0.5 MPa. The dielectric constant values, measured at 0.5 MPa, are 14.30 and 14.08 for sample c-1 and 14.17 for sample c-2. These values are higher than those obtained previously and may result from a thicker film.

Three samples have been tested in the fourth configuration. The results for the g constant are plotted in Fig. 10—the solid lines at the bottom marked d-1, d-2, and d-3. The dielectric constants at a pressure of 0.5 MPa are 13.47, 12.93, and 13.64, respectively.

The results presented in these last two sections show variation in the piezoelectric and dielectric constants. These variations may be caused by inhomogeneous polarization of the PVF_2 or variations of thickness across the film, or both. Another factor that can cause variations in the dielectric constant is the shrinkage of the film when it is in contact with the castor oil [26]. This effect is small, however, and the total change in area is probably less than 2%. It is believed that for the case of the two-sided clamping, described by the first configuration, or for that of the one-sided clamping, described by the second and third, this effect of shrinkage is negligible due to the differences in the elastic compliance of the PVF_2 and the stainless-steel. Another reason for the difference in the dielectric constant

for the various configurations may be the electric field structure near the edges of the film caused by the electrodes' geometry. This field distortion causes changes in the capacitance readings compared to the "perfect sample" and hence in its dielectric constant.

The results obtained for g in the second configuration (the b curves of Fig. 10) are higher than those in the third one (the c curves of Fig. 10). The number of samples tested is too small to make conclusions about the average value and variations from the average in each of the configurations. However, it is clear that the fourth configuration (the d curves) with no rigid backing, has the lowest sensitivity. The first configuration (the a curve) represents the fully clamped case and the fourth configuration (d curves) represents the freely suspended case; all other cases are in-between. It is expected that the value of the piezoelectric coefficient for any other configuration will be bounded between these extreme curves.

RECEIVING RESPONSE AS A FUNCTION OF FREQUENCY

With the coupler, it is possible to find the response of the PVF₂ hydrophone by driving one of the ceramic spheres, monitoring a constant sound pressure level (constant output voltage if the response is flat) with the other sphere, and measuring the output voltage of the PVF₂ sample. In the experiments to be described, the monitoring voltage was 0.025 V and the hydrostatic pressure was 1 MPa.

The samples used for frequency response testing were sample c-1 with stainless-steel backing and sample d-3 with no backing; both were tested at 25°C. The relative receiving voltage of the hydrophone for each sample is plotted in Fig. 11. The response was measured in the range of 50 to 2000 Hz and is practically flat. Notice the response of the fully suspended sample d-3 which is less than that of the other one. This result is in accordance with that reported in the previous section.

TRANSMITTING RESPONSE AS A FUNCTION OF FREQUENCY

The experimental setup used for measurement in the receiving mode can also be used for determining the transmitting characteristics of PVF₂. With driving voltage applied to the PVF₂ sample, the output voltage produced by each of the ceramic spheres can be recorded. In this case, the PVF₂ sample serves as a projector P and the spheres as transducer T and hydrophone H. Thus, with the assumption of reciprocity of the PVF₂ in the coupler, the sound pressure level (SPL) produced by the PVF₂ can be evaluated. This evaluation can be compared with the SPL as measured by the hydrophone.

Let us first calculate the SPL that should be produced by the PVF₂ with the assumption of reciprocity. The basic equations are [23]:

$$TCR = \frac{M_o}{J} , \quad (3)$$

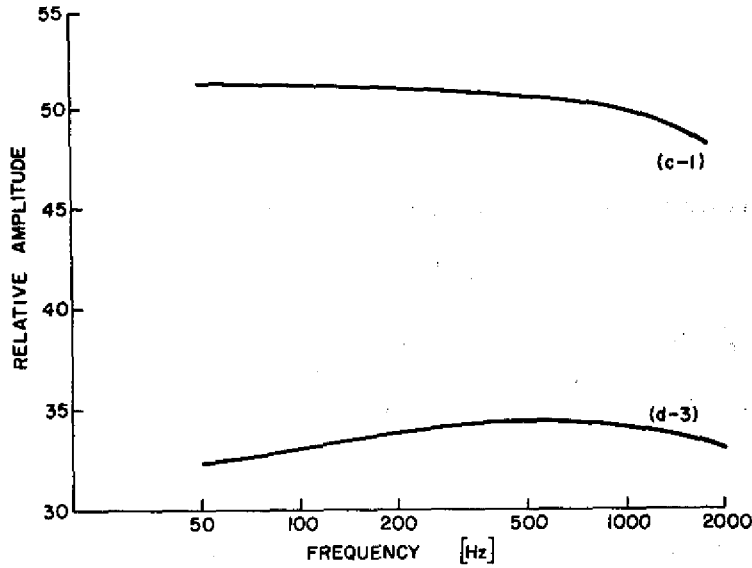


Fig. 11 — Relative receiving voltage of PVF₂ samples as a function of frequency at 25°C

and

$$TVR = \frac{TCR}{Z}, \quad (4)$$

where: *TCR* is transmitting current response,
TVR is transmitting voltage response,
M_o is free-field voltage sensitivity,
J is reciprocity parameter, and
 $Z = \frac{1}{\omega C}$ electrical impedance.

The reciprocity parameter *J* for the coupler is given by:

$$J = \frac{2\pi fV}{\rho c^2} = 3.86 \times 10^{-10} \text{ VA/Pa}^2, \quad (5)$$

where *f* is frequency (*f* = 1000 Hz),
V is coupler's volume (*V* = 146.9 × 10⁻⁶ m³),
ρ is density of castor oil (*ρ* = 971 kg/m³), and
c is speed of sound in castor oil (*c* = 1570 m/s).

Hence,

$$TCR = 7135 \text{ [Pa/A]}, \quad (6)$$

and

$$TVR = 0.0259 \text{ [Pa/V]}. \quad (7)$$

For an applied driving voltage of 96.2 V the calculated *SPL* produced by the PVF₂ is

$$SPL_{\text{calc.}} = 2.489 \text{ Pa}. \quad (8)$$

Let us now calculate the measured *SPL* incident on one of the receivers. Its sensitivity is $M_p = 199.0 \text{ dB re } 1 \text{ V}/\mu\text{Pa}$ or $M_p = 1.119 \times 10^{-4} \text{ V/Pa}$. The output voltage of the receiver is $e'_{HP} = 2.395 \times 10^{-4} \text{ V}$ and, therefore

$$SPL_{\text{meas.}} = 2.140 \text{ Pa}. \quad (9)$$

This measured result is in reasonable agreement with that calculated from the PVF₂ characteristics. Preliminary measurements have shown that the film is linear for driving fields up to $3.7 \times 10^6 \text{ V/m}$.

The output voltage of each of the spheres divided by the driving voltage of the PVF₂ sample c-1 is plotted in Fig. 12 as a function of frequency for 25°C and a hydrostatic pressure of 1 MPa. The range is 200 to 2000 Hz; because of noise problems, it was difficult to measure below 200 Hz. The variation of the measured response from an average curve is less than ±2%. These variations include error due to the experimental uncertainty. This average curve agrees well with a curve calculated from the *J* parameter and the sensitivities of the PVF₂ and of the sphere.

EVALUATION OF THE PRE-POSFET PIEZOELECTRIC TRANSDUCER

The mechanical and piezoelectric properties of PVF₂ have been described earlier. It had been found that PVF₂ has some advantages over ceramics being used in acoustic applications. Work at Stanford University has demonstrated the substantial promise of PVF₂ for high-frequency medical imaging and nondestructive testing systems in the 1- to 20-MHz frequency range. These investigators developed an integrated PVF₂-Si transducer—the POSFET (piezoelectric-oxide semiconductor, field effect transistor), which is described in [17-19].

A modification of the POSFET is a PVF₂-on-sapphire transducer that was developed and assembled by the Integrated Circuits Laboratory, Department of Electrical Engineering, at Stanford University. These transducers consist of the PVF₂ and the sapphire only and do not contain any active electronics. This configuration has been named "pre-POSFET." The first pre-POSFET samples were prepared by cementing a commercial PVF₂, supplied by Kureha Chemical Industry Co., that had aluminum electrodes to the sapphire substrate that

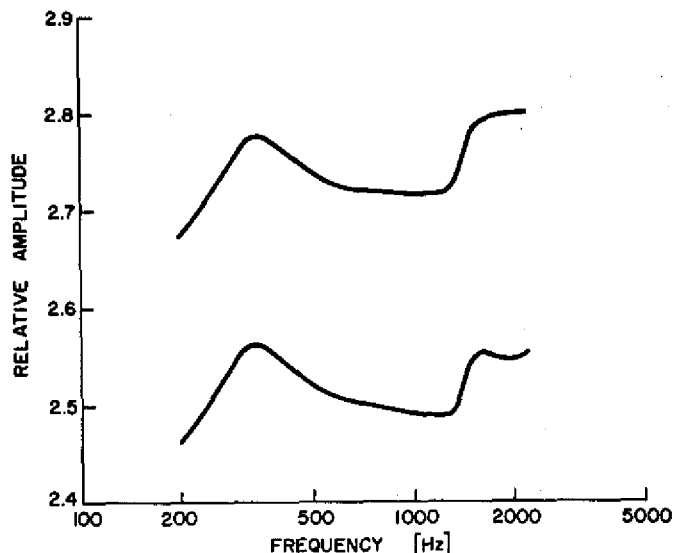


Fig. 12 — Relative output voltage as a function of frequency of the ceramic spheres when sound is generated by NRL-USRD (c-1) PVF₂ sample at 25°C and 1 MPa

had nickel metallization on it. The electrical connection to the top electrode was made with gold wire cemented with conductive silver-filled epoxy. These samples had unreliable wire contacts to the aluminum electrodes.

The second set of samples was assembled as follows [27]: the metallization pattern on the sapphire was nickel as in the first batch. The PVF₂ itself had no bottom electrode and was mounted with a nonconductive epoxy on the nickel pad, which served as the bottom electrode. The top electrode on the PVF₂ was chrome-gold, and the metallization was done with a sputtering technique. After the Cr-Au deposition, the PVF₂ was reepoled (at Stanford). Connections to the top electrode were made with gold wires and a conductive Ag-filled epoxy. Each sample had two sets of wires. The entire structure was coated with parylene for waterproofing.

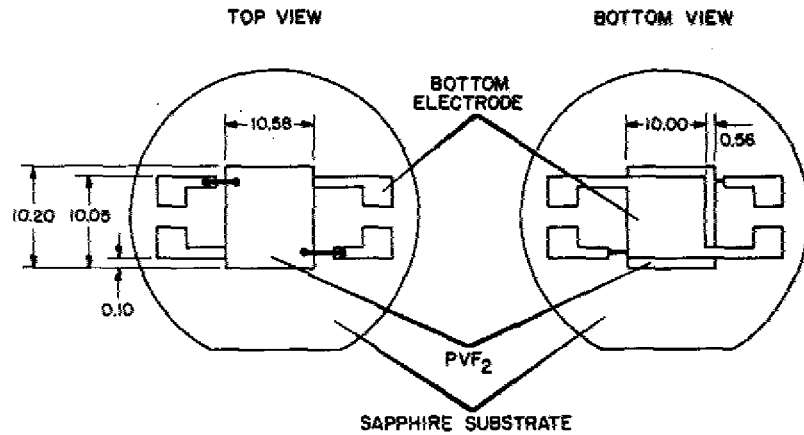
This section summarizes NRL-USRD's evaluation of these pre-POSFET samples.

Dimensions

Three samples were obtained from Stanford University and used in this part of the investigation. The thickness of the sapphire was 3.05×10^{-4} m and its diameter 4×10^{-2} m. The thickness of the PVF₂ was not measured but was assumed to be 27 μ m. Because the PVF₂ was cemented with nonconductive epoxy, the measured capacitance of the sample was smaller than the actual capacitance of the PVF₂ and was dependent on the thickness of the cement layer.

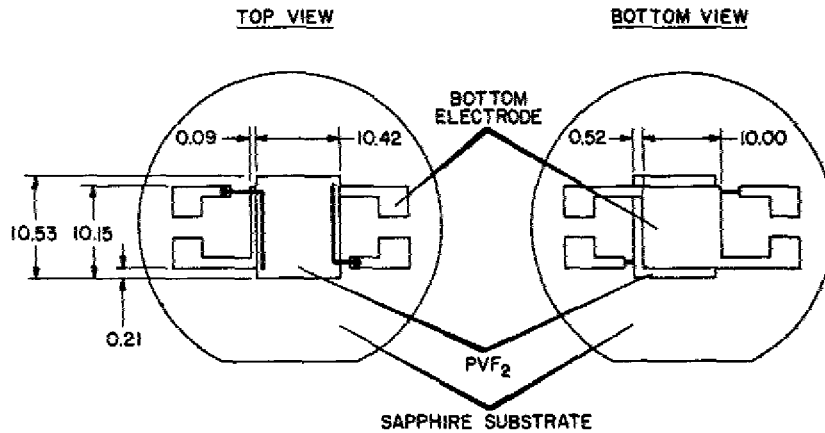
BERLINSKY

The description and dimensions of the samples marked as 5, 6, and 7 are presented in Figs. 13, 14, and 15, respectively. The area of the PVF_2 is greater than that of the bottom electrode. In sample 5 the film covers all the bottom electrode area (see Fig. 13). Part of the bottom electrode in sample 6 is not covered by the PVF_2 (see Fig. 14). In sample 7 the PVF_2 is rotated relative to the electrode (see Fig. 15). Since there is no conducting path between the PVF_2 and the lower electrode, the area was taken to be the overlapping area.



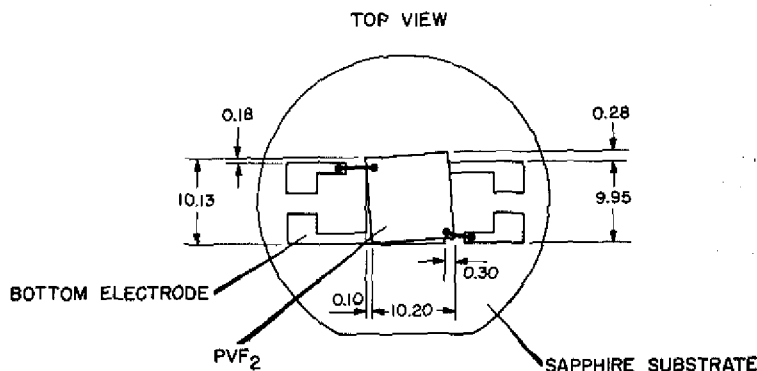
NOT TO SCALE - DIMENSIONS IN mm.

Fig. 13 - Description of pre-POSFET sample 5



NOT TO SCALE - DIMENSIONS ARE IN mm.

Fig. 14 - Description of pre-POSFET sample 6



NOT TO SCALE - DIMENSIONS IN mm.

Fig. 15 — Description of pre-POSFET sample 7

Capacitance and Dissipation Factors

The capacitance and dissipation factors were measured with a digital capacitance meter at 1000 Hz and are presented in Table 1. The results measured by each of the two sets of leads are the same, indicating a good wire contact to the PVF₂. It was confirmed by the zero resistance between the two leads connected to the top electrode.

Table 1 — Capacitance and Dissipation Factors at 1000 Hz

Sample No.	C(pF)	D
5	376.5	0.0233
6	405.5	0.0177
7	418.0	0.0660

The dissipation factor of sample 7 is too high, compared with the other two samples and values obtained at NRL-USRD or given by the Kureha Chemical Industry Co. or other researchers. The difference in the samples' capacitances could be either because of thickness differences in the PVF₂ or in the nonconductive epoxy, or both.

Receiving Response of the Pre-POSFET Configuration

The method used for determining the piezoelectric constants in the coupler reciprocity method was described earlier. The projector (transmit only) is a ceramic sphere

($C \approx 11,100$ pF), the transducer (transmit and receive) is a ceramic sphere ($C \approx 5200$ pF), and the hydrophone is the PVF_2 - sapphire sample.

Sensitivity as a Function of Hydrostatic Pressure — Sample 5

This measurement was taken at 25°C and 1000 Hz. The sapphire was mounted on the coupler plug with four supporting pins. The configuration is shown in Fig. 16a and is labeled "unbacked." When the coupler was filled with castor oil, the capacitance was about 5% less than before. The dissipation factor was relatively low—0.0132.

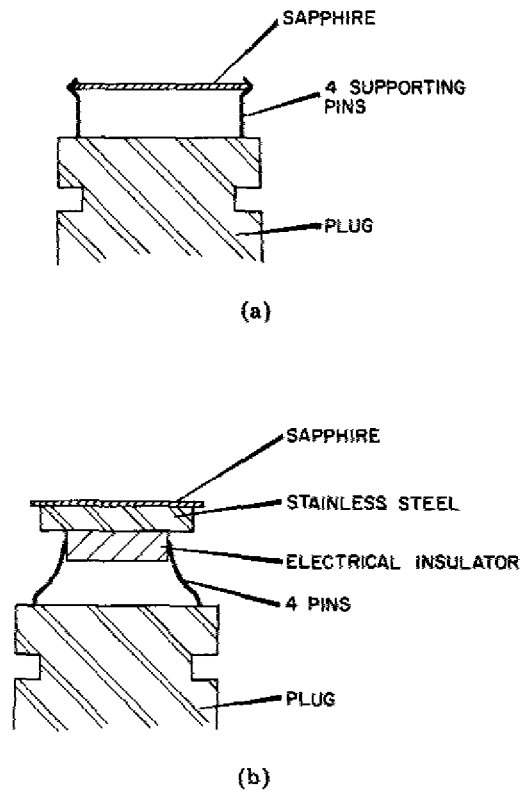


Fig. 16 — "Backed" and "unbacked" configurations for mounting the pre-POSFET samples

As explained in the section entitled CALIBRATION WITH THE RECIPROcity COUPLER, the calibration gives the free-field voltage sensitivity, and hence g . Through K_{33}^T , d (the hydrostatic piezoelectric strain coefficient) is computed. Results for g , K_{33}^T , and d for sample 5 as a function of hydrostatic pressure are plotted in Fig. 17. The general behavior is similar to that obtained with the samples discussed in the section entitled PIEZOELECTRIC VOLTAGE COEFFICIENT FOR PVF_2 IN VARIOUS

CONFIGURATIONS SUBJECTED TO HYDROSTATIC PRESSURE, which were not of the pre-POSFET configuration, although the values of g , K_{33}^T , and d in Fig. 17 are smaller.

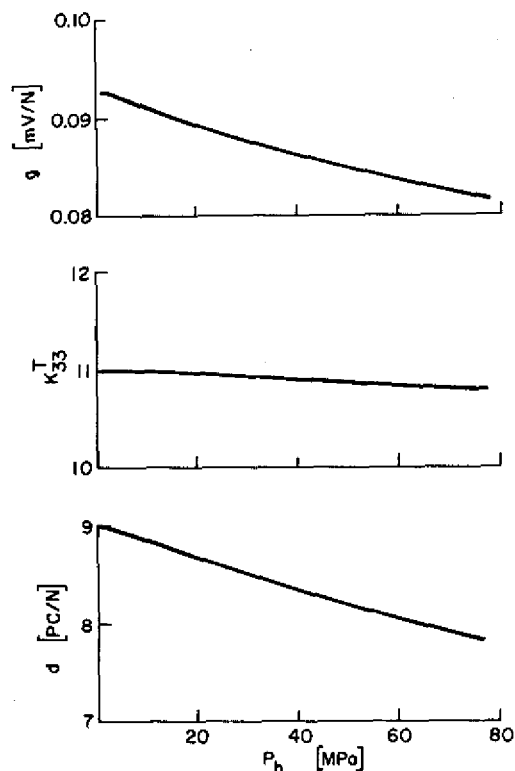


Fig. 17 — Sample 5 — g , K_{33}^T , and d as a function of hydrostatic pressure

Frequency Response — Sample 5

The same method described in the section entitled RECEIVING RESPONSE AS A FUNCTION OF FREQUENCY was used to determine the receiving response of the pre-POSFET samples.

The relative receiving voltage of sample 5, as a function of frequency at 25°C and at a hydrostatic pressure of 1 MPa, was measured and plotted in Fig. 18 (solid line). It is seen that the response is not flat, and there are resonances at relatively low frequencies. These resonances seem to originate from flexural modes of vibration of the sapphire substrate.

A complete reciprocity calibration was made in order to verify these results. A plot of the apparent g is given in Fig. 19. Although there is a difference in the fine structure, the general behavior is the same as described in Fig. 18. The changes in the fine structure are due to changes in the monitor's sensitivity within the experimental uncertainty.

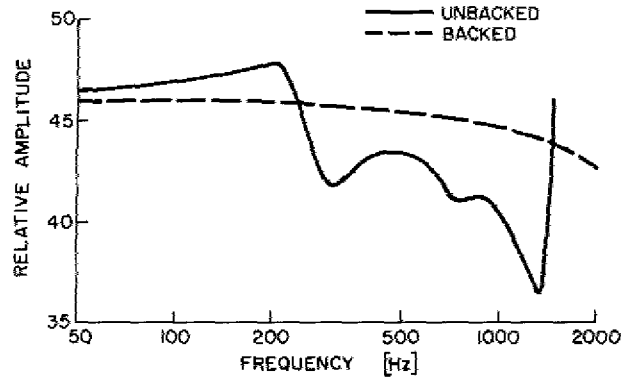


Fig. 18 — Sample 5 — relative receiving voltage as a function of frequency at 25°C and 1 MPa

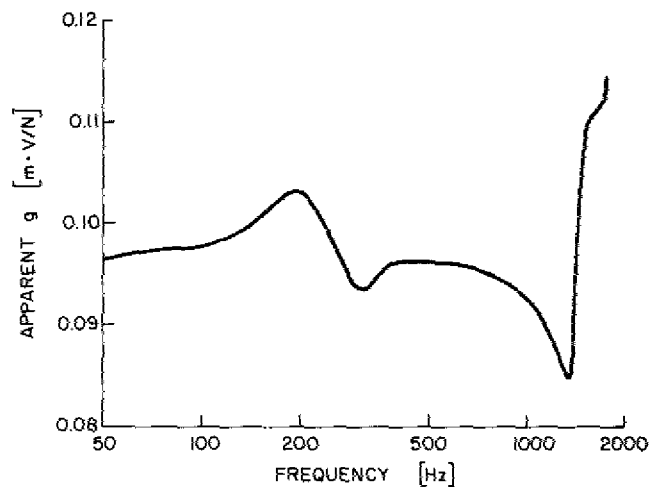


Fig. 19 — Sample 5 — apparent piezoelectric voltage coefficient as a function of frequency

Data obtained from sample c-1, Fig. 11, have shown a flat response when the $PV F_2$ film was cemented to a rigid substrate such as a thick disc of stainless-steel. To duplicate those conditions in this case, the sapphire was cemented with Alpha-cement to a stainless-steel disc 5×10^{-3} -m thick and 35×10^{-3} m in diameter. This configuration is named "backed" and is described in configuration b of Fig. 16. The relative receiving voltage in the "backed" configuration as a function of frequency is shown in Fig. 18 as a dashed line. The resonance modes have been completely damped, and the response is flat.

Frequency Response -- Sample 6

The procedure described in the section entitled RECEIVING RESPONSE AS A FUNCTION OF FREQUENCY was also used for evaluating the response of sample 6. The sample was mounted unbacked as described in configuration a of Fig. 16 and tested at a temperature of 25°C and a hydrostatic pressure of 1 MPa.

A relative receiving voltage of the hydrophone is plotted vs. frequency in Fig. 20. The solid line represents the case where the sapphire was simply supported by the pins. The dashed line is the case when it was cemented with Alpha-cement to the same pins. The dash-dot line corresponds to a case where unbacked sample is cemented to more rigid pins.

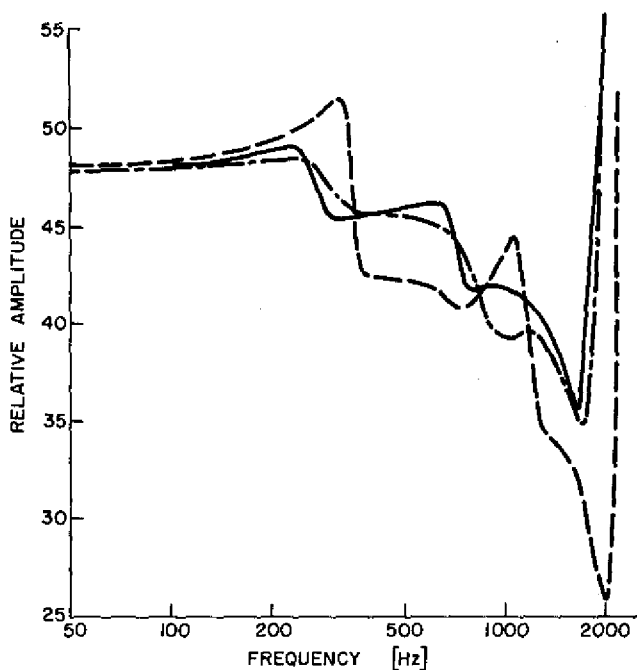


Fig. 20 -- Sample 6 -- relative receiving voltage as a function of frequency

The frequency response of sample 6 can be seen to be similar to that of sample 5. Changing the way of mounting causes some changes in the fine structure of the response although the general structure of the curves remains unchanged. Sample 6 was not evaluated in the "backed" configuration.

Frequency Response of NRL-USRD Pre-POSFET Sample

After data were obtained from Stanford's pre-POSFET transducers, a specimen was prepared as hereby described. The parylene cover of one of the sapphire samples (thickness of the sapphire—0.36 mm) of the first batch received from Stanford was removed together with the PVF₂ film. The nickel metallization remained undamaged and served as the bottom electrode. A square piece of PVF₂ was cemented on top of the bottom electrode using a conductive silver-filled epoxy. Electrical contacts to the top electrode were made by means of gold leaves and conductive gold-filled epoxy. The sample was cemented with Alpha-cement to the four pins (as shown in configuration a of Fig. 16, and was tested at 25°C and at hydrostatic pressure of 1 MPa.

Relative receiving voltage as a function of frequency is presented in Fig. 21. The response is generally the same as those of samples 5 and 6. This is an indication of the repeatability of samples with similar characteristics.

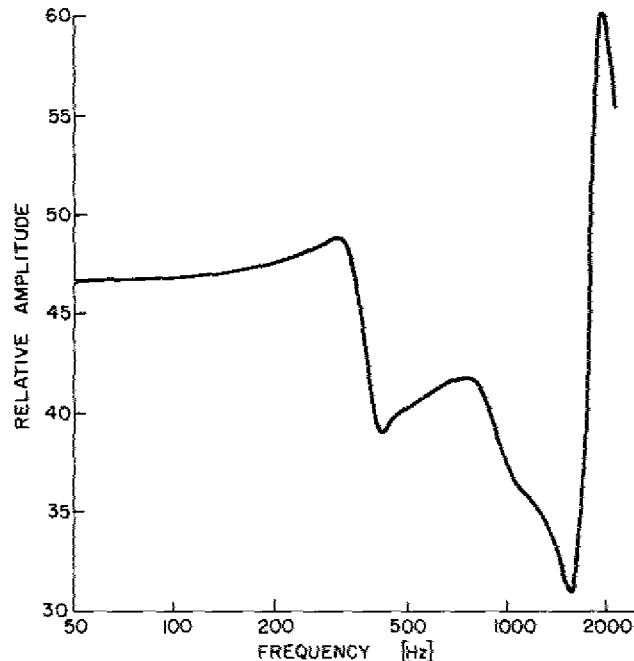


Fig. 21 — NRL-USRD pre-POSFET sample—relative receiving voltage as a function of frequency

Frequency Response of PZT-4 on Sapphire

Another sapphire substrate from the first batch from Stanford was utilized to construct the following transducer. After removal of the parylene cover and the PVF₂ film,

a thin ceramic PZT-4 disc was cemented to the sapphire with conductive silver-filled epoxy. The ceramic thickness was 0.3×10^{-3} m, and its diameter was 12.7×10^{-3} m. Electrical connections to the top electrode were made using gold leaves and conductive silver-filled epoxy.

The temperature and pressure conditions were the same as before. A plot of the relative receiving voltage as a function of the frequency is presented in Fig. 22. There is a difference between this response and that of the PVF₂ on sapphire samples. Yet even here two clear resonances exist, and they are much more intense. The difference may be related to the difference in the elastic compliance of PVF₂ and PZT-4, which changes the rigidity of the hydrophone, and not necessarily because of inhomogeneous polarization in the PVF₂. The polarization in the PZT is homogeneous.

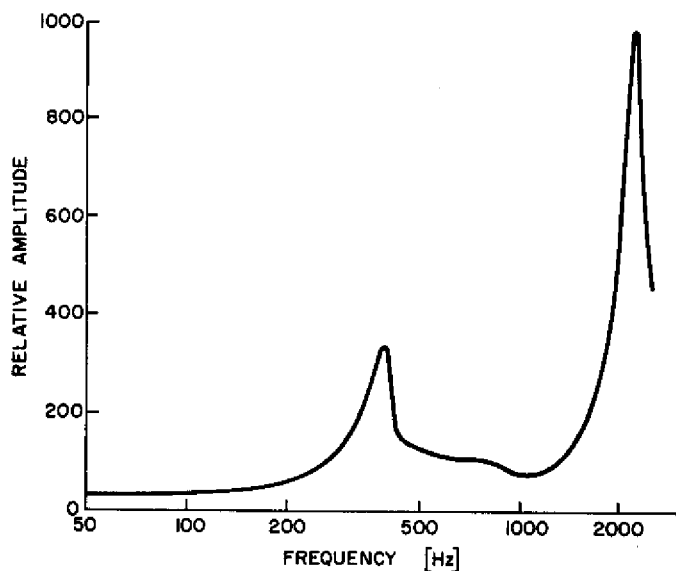


Fig. 22 — PZT-4 on sapphire sample — relative receiving voltage as a function of frequency

Transmitting Response of the Pre-POSFET Configuration

The method used for evaluating the transmitting response of the pre-POSFET transducers was described in the section titled TRANSMITTING RESPONSE AS A FUNCTION OF FREQUENCY. Let us first calculate the SPL produced by the pre-POSFET sample 5 (unbacked), at 25°C and hydrostatic pressure of 1 MPa, by using Eqs. (3), (4), and (5). With the following values, $V = 151.7 \times 10^{-6}$ m³, $f = 1000$ Hz, $\rho = 971$ kg/m³, and $c = 1570$ m/s, we obtain $J = 3.982 \times 10^{-10}$ [VA/Pa]². Hence:

$$TCR = 6295 \text{ [Pa/A]}, \quad (10)$$

and

$$TVR = 0.01419 [Pa/V]. \quad (11)$$

When a driving voltage of 100 V is applied, the calculated SPL produced by sample 5 is

$$SPL_{calc.} = 1.419 Pa. \quad (12)$$

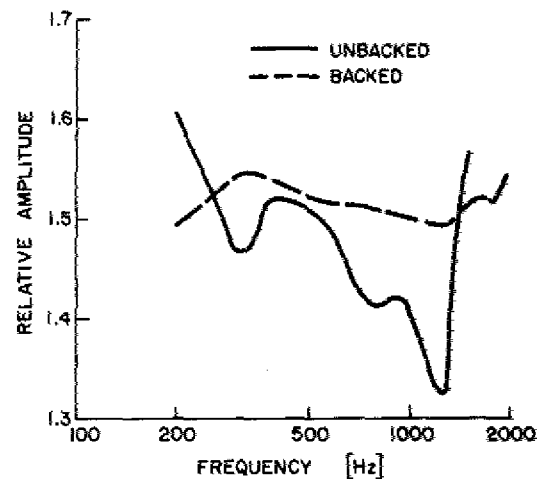
Now compare $SPL_{calc.}$ with the measured value; the sensitivity of the receiver is $M_p = -199.0$ dB re 1 V/ μ Pa or $M_p = 1.119 \times 10^{-4}$ V/Pa. The output voltage of the receiver is $e'_{HP} = 1.41 \times 10^{-4}$ V and, therefore,

$$SPL_{meas.} = 1.26 Pa, \quad (13)$$

which is in reasonable agreement with the result evaluated from the PVF_2 characteristics.

The relative output voltage of the ceramic sphere divided by the driving voltage of sample 5 is plotted in Fig. 23 as a function of frequency at 25°C and hydrostatic pressure of 1 MPa. The solid line represents the unbacked case while the dashed line represents the backed configuration. It is seen that even in the transmitting mode there are resonances at relatively low frequencies that are damped when the sapphire substrate is cemented onto a rigid backing.

Fig. 23 — Relative output voltage as a function of frequency at 25°C and 1 MPa of a ceramic sphere when sound is generated by pre-POSFET sample 5



Discussion

The problem of making reliable wire contacts to the pre-POSFET samples has been adequately solved by using the procedure developed at Stanford University that was described in an earlier section.

The use of nonconductive epoxy for cementing the PVF₂ on the sapphire substrate inserts a capacitance in series with the film. It causes a decrease in the output voltage and, hence, in the free-field voltage sensitivity. The thickness of this layer is uncontrolled, resulting in changes in the sample's sensitivity. Other causes for the sensitivity variations can be inhomogeneous polarization across the film and variation in its thickness.

The pre-POSFET samples (as received from Stanford) exhibit low-frequency resonances in both the receiving and the transmitting modes of operation. These resonances are due to flexural mode vibrations of the sapphire substrate. When cemented onto a rigid backing, these low-frequency resonances disappear.

HIGH AMPLITUDE DYNAMIC STRESS TRANSDUCER

Calibration and characterization of PVF₂ in the hydrophone mode of operation have been described in the previous sections. In the previous sections the hydrophone is subjected to a hydrostatic pressure (which may result in a one-dimensional stress on the film itself) and is activated by a sinusoidal sound pressure field (small amplitude).

A second way of calibration or characterization is in the dynamic pressure transducer mode. The sensor is loaded by a single pressure pulse whose amplitude is much greater than that of an ordinary sound pressure. Such pulses arise from shock waves in water or from pressure in the interface of colliding objects. The calibration is done using a comparison method. A standard pressure transducer and the hydrophone are mounted in a pressure cell. The cell (Fig. 24) is filled with a fluid having high electrical resistivity (castor oil) and is dynamically loaded by a drop weight that hits the piston.

The charge produced by each of the two sensors is converted to voltage with a charge amplifier and is recorded. The sensitivity is computed from the sensitivity of the standard and the setting of the electronic system. The pressure cell is temperature controlled.

The sample was the same as used in the coupler calibration, marked sample 1. The effective d_{33} is directly calculated as the charge per unit area produced by the PVF₂ divided by the pressure measured with the standard sensor and the area ratio. A calibrated quartz transducer (PCB Piezotronics Model 116A03) is used as the standard. Figure 25 shows effective d_{33} as a function of peak dynamic one-dimensional stress for four temperatures: 40, 25, 15, and 4.5°C. In these measurements the rise time of the pulse was approximately 3500 μs. The change of d_{33} with peak stress at 4.5°C is about 10% (0.8 dB) and is smaller for elevated temperatures. For practical use, results can be approximated by a straight line, and the error will be less than ±3% (0.25 dB).

One of the tests for sonar transducers is the ability to withstand an explosive shock wave loading having a peak pressure of about 3500 psi (~25 MPa). Under such a loading, PVF₂ is almost unaffected and up to this pressure its sensitivity in the one-dimensional configuration as a pressure sensor would change only 0.3 dB.

PRESSURE CELL
FOR DYNAMIC
CALIBRATION

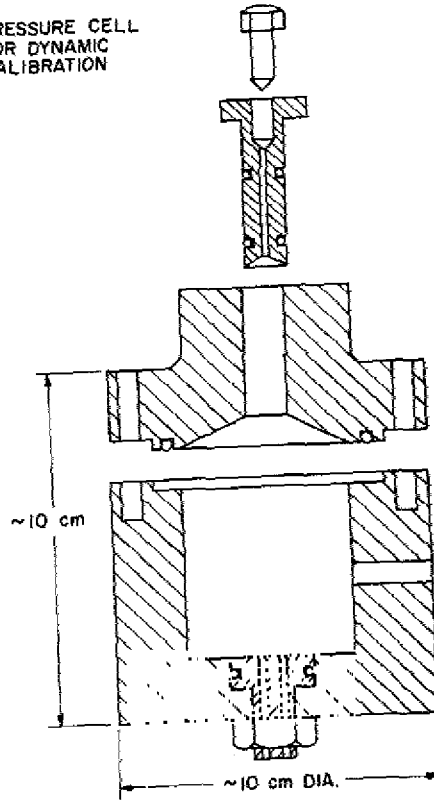


Fig. 24 — Cross section of a dynamic pressure cell

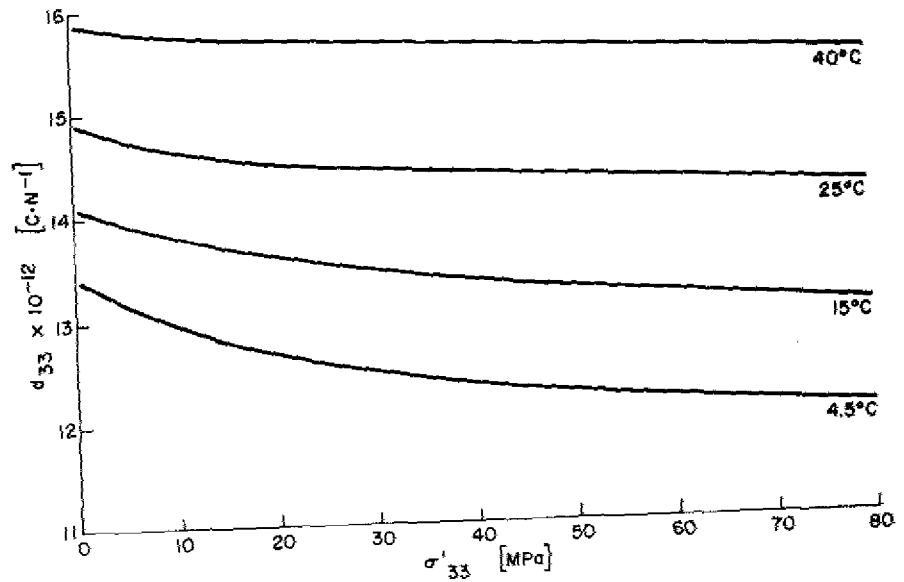


Fig. 25 — Effective piezoelectric strain coefficient as a function of peak dynamic one-dimensional stress for four temperatures

A second, smaller pressure cell with internal dimensions of 1.1×10^{-2} -m diam and 1.1×10^{-2} -m high has been used to get pressure pulses with a shorter rise time. The operation is the same as with the first cell. Changing the drop weight causes changes in the rise time.

Three samples have been tested with the second pressure cell. They are described in Fig. 26. The first, sample *e*, is constructed from a circular sheet of PVF₂ cemented on a brass disc with conductive silver-filled epoxy. Part of the PVF₂ near the edge, which was cemented improperly, has been cut off. The area of the PVF₂ is 3.7×10^{-5} m². The second, sample *f*, is the same as the first one, but the PVF₂ is completely circular and has an area of 3.85×10^{-5} m². The third, sample *g*, is a freely-suspended (unbacked) circular sheet of PVF₂ having an area of 3.85×10^{-5} m². Electrical connections have been made with gold leaves and conductive gold-filled epoxy.

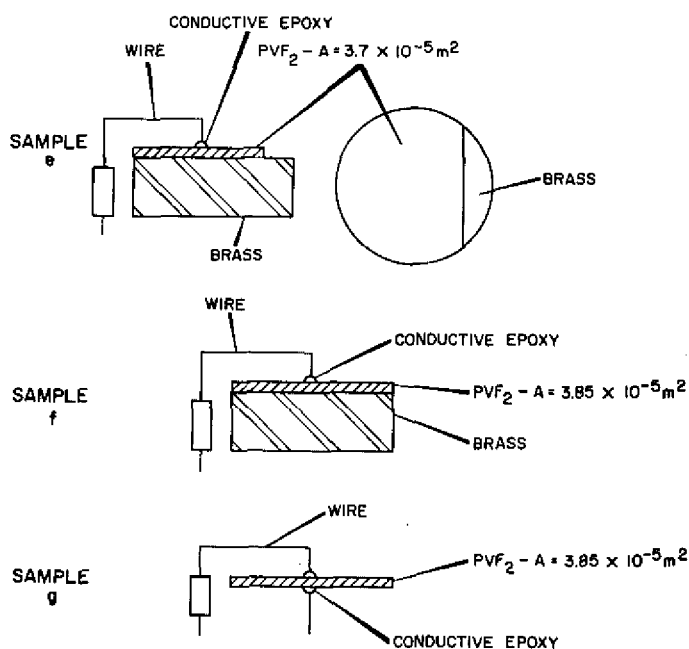


Fig. 26 — Configurations for dynamic pressure calibrations on three samples

The samples described above were used to measure the linearity of the PVF₂ with peak dynamic pressure and its response to dynamic loading having different rise times. All tests were conducted at 25°C.

The measured *d* constant as a function of peak dynamic hydrostatic pressure for sample *e* is described in Fig. 27. The plot *e*₁ corresponds to a peak loading having a rise time of about 900 μs and *e*₂ of about 200 μs. These results indicated that the *d* constant is

dependent on the rise time. Therefore tests have been conducted in which the peak pressure was almost the same (~ 10 MPa) and the rise time was changed. It is not critical to get exactly 10 MPa for each shot, since d is almost constant with peak pressure, as shown in Fig. 27.

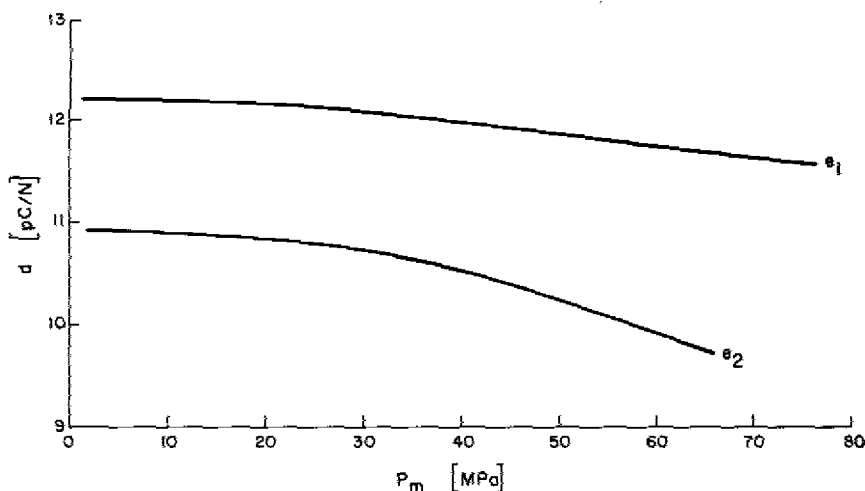


Fig. 27 — Measured piezoelectric strain coefficient as a function of peak dynamic hydrostatic pressure (e_1) — rise time $\sim 900 \mu s$, (e_2) — rise time $\sim 200 \mu s$

The d as a function of pulse rise time is shown in Fig. 28 for the three configurations. The difference between samples e and f is 10 to 15%. Variations in the d value can be explained as a result of variations in the thickness. The same variations in d value were obtained with the coupler reciprocity method (see sections entitled PIEZOELECTRIC CONSTANTS — ONE DIMENSIONAL CONFIGURATION and PIEZOELECTRIC VOLTAGE COEFFICIENT FOR PVF_2 IN VARIOUS CONFIGURATIONS SUBJECTED TO HYDROSTATIC PRESSURE). The d value for the g configuration of Fig. 26 is significantly lower due to the hydrostatic nature of the stress acting on the film.

Attention has to be paid to the fact that the rise time is amplitude dependent, especially in low-amplitude loading where the rise time is longer.

Results presented in Fig. 28 show lower values of d than for the sample described in Fig. 2 (see the data of Fig. 6). There is a tendency for the g constant to decrease when a sample with smaller area is used (clamped on one side — see Fig. 9 configuration c). It is believed that there exists a section of the PVF_2 film near its edge where the material behaves as if it were unclamped. As the film area is reduced, the ratio of the area of this unclamped region to the total area becomes closer to one. Hence, the film is coming nearer to the state of the freely suspended sample (unbacked). This can explain in part the difference in results obtained for the sample used with the first pressure cell and sample e used with the second one (together with the difference in rise time in the two cases).

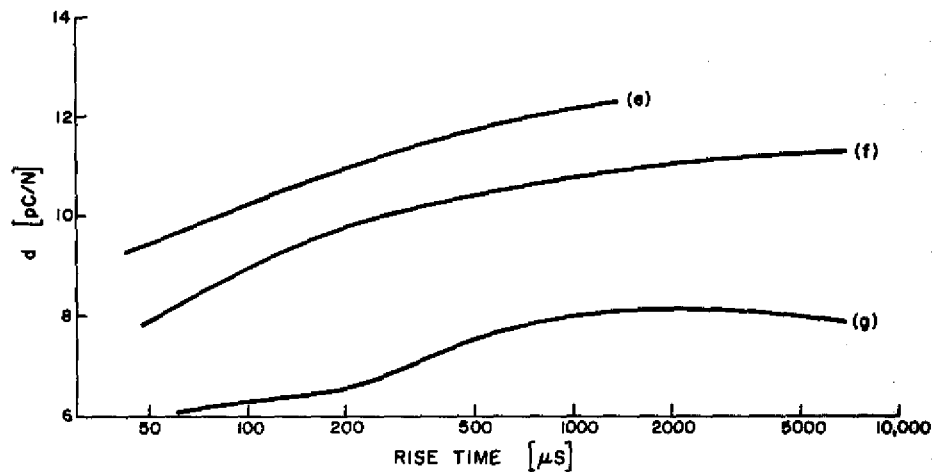


Fig. 28 — Piezoelectric strain coefficient as a function of pulse rise time for three configurations

SUMMARY

This report presents the basic piezoelectric properties of PVF_2 and their pressure, frequency, and temperature dependencies. Some of these properties show improved behavior of the piezopolymer over piezoceramics used in sonar applications.

Tests have been performed on PVF_2 in various configurations as a function of temperature, frequency, and stress. The PVF_2 was operated both as a hydrophone and as a projector. Results of these tests have been presented and discussed.

These results show that g is relatively high and d is relatively small compared with typical ceramics. This indicates that a PVF_2 transducer will be more suitable as a hydrophone than as a projector. However, the transmitting capability of PVF_2 has been demonstrated for relatively low driving voltage. Since the dielectric strength is high and thickness is small, it is possible with a driving voltage of the order of 1 kV to obtain a very large electric field and, therefore, a reasonable SPL.

Samples prepared from the same sheet of PVF_2 exhibit variations in the piezoelectric activity. The number of tests conducted on each configuration is too small to determine an average value and the variations from this average; yet, it is clear that samples clamped on two sides, or even one, exhibit greater sensitivity in the thickness mode of operation than those that are freely suspended in a hydrostatic environment. The existence of variation in results for a given configuration indicates that each device to be constructed and used will have to be calibrated separately.

The d constant of quartz and tourmaline is about 2×10^{-12} C/N; therefore, a PVF_2 gauge having the same area would have a sensitivity about seven times greater. Moreover,

because of its very small thickness, it would have a better frequency response and would record blast waves more accurately.

These results, among others to be obtained in the future, characterize the material. They will enable the design, construction, and testing of devices to be used in acoustics and other dynamic pressure applications.

ACKNOWLEDGMENT

The author wishes to express gratitude to all the employees of NRL-USRD for their contributions which led to a pleasant and stimulating stay there. Special thanks are expressed to Dr. R. W. Timme for making this research possible; to Messrs. L. P. Browder, S. W. Meeks, and L. A. Boles for their consulting assistance and suggestions, especially that concerning the coupler reciprocity calibration method; to Mr. E. W. Thomas for his help with the instrumentation; to Mr. G. D. Hugus for design of the dynamic pressure cell; and to Messrs. R. J. Powelson and F. W. Schimmel for designing and constructing the charge amplifier.

REFERENCES

1. W.G. Cady, *Piezoelectricity*, Dover Publications, Inc., New York (1964).
2. E. Fukada, "Piezoelectricity of Wood," *J. Phys. Soc. Japan* **10**, 149 (1955).
3. E. Fukada, M. Date, and K. Hara, "Temperature Dispersion of Complex Piezoelectric Modulus of Wood," *Japanese J. Appl. Phys.* **8**, 151 (1969).
4. E. Fukada and I. Yasuda, "On the Piezoelectric Effect of Bone," *J. Phys. Soc. Japan* **12**, 1158 (1957).
5. S. Edelman and D.E. Gilbert, "Evaluation of Polarized Materials for Sonar Transducers," Research Triangle Institute (1975).
6. H. Kawai, *Japanese J. Appl. Phys.* **8**, 975 (1969).
7. G.T. Davis, J.E. McKinney, M.G. Broadhurst, and S.C. Roth, "Electric-Field-Induced Phase Changes in Polyvinylidene Fluoride," *J. Appl. Phys.* **49**(10), 4998-5002 (1978).
8. E. Fukada, "Piezoelectric Polymers and Their Application," Proceedings of the 2nd Meeting on Ferroelectric Materials and Their Applications, Kyoto, May 1979.
9. M.G. Broadhurst, G.T. Davis, J.E. McKinney, and R.E. Collins, "Piezoelectricity and Pyroelectricity in Polyvinylidene Fluoride - A Model," *J. Appl. Phys.* **49**(10), 4992-4997 (1978).
10. N. Murayama, K. Nakamura, H.O. Bara, and M. Segawa, "The Strong Piezoelectricity in Polyvinylidene Fluoride (PVDF)," *Ultrasonics* **14**, 15-23 (January 1976).
11. R. Hayakawa and Y. Wada, *Adv. Polym. Sci.*, **11**, 1 (1973).

12. H. Sussner and K. Dransfeld, "Importance of the Metal-Polymer Interface for the Piezoelectricity of Polyvinylidene Fluoride," *J. Polym. Sci., Polymer Physics Edition*, Vol. 16, 529-543 (1978).
13. T.D. Sullivan and J.M. Powers, "Piezoelectric Polymer Flexural Disk Hydrophone," *J. Acoust. Soc. Am.* 63(5), 1396-1401 (May 1978).
14. J.F. Kilpatrick, Jr., "Piezoelectric Polymer Cylindrical Hydrophone," Presentation at the 96th Meeting of the Acoust. Soc. of Am. in Honolulu, Hawaii (November 1978).
15. N. Chubachi, "Piezoelectric Polymer Transducer and Its Application to Acoustics," Presentation at the 96th Meeting of the Acoust. Soc. of Am. in Honolulu, Hawaii (November 1978).
16. P.E. Bloomfield, "Piezoelectric Polymer Transducers for Detection of Structural Defects in Aircraft," AD A055 729.
17. J.D. Plummer and J.D. Meindl, "Fabrication, Characterization, and Optimization of POSFET (PVF₂-Silicon) Piezoelectric Transducers for Low Frequency (100 Hz to 500 kHz) Underwater Acoustic Applications," A proposal to the Naval Research Laboratory, USRD (July 1978).
18. R.G. Swartz and J.D. Plummer, "Monolithic Silicon-PVF₂ Piezoelectric Arrays for Ultrasonic Imaging," Presentation at the 8th International Symposium on Acoustic Imaging, Key Biscayne, Fla. (1978).
19. R.G. Swartz, "Application of Polyvinylidene Fluoride to Monolithic Silicon/PVF₂ Transducer Arrays," Sel-79-013, Technical Report No. G561-1, Stanford Electronics Laboratory, May 1979.
20. A.S. DeReggi, "Piezoelectric Polymer Transducer for Impact Pressure Measurement," NBSIR 75-740, July 1975.
21. P.E. Bloomfield, "Piezoelectric Polymer Films for Fuze Applications," NBSIR 75-724(R), Aug. 1975.
22. W.H. Chen *et al*, "PVF₂ Transducers for NDE," 1978 Ultrasonics Symposium Proceedings.
23. R.J. Bobber, *Underwater Electroacoustic Measurements*, Naval Research Laboratory (Government Printing Office, Washington, DC, 1970).
24. L.A. Boles, "Correction Factors for a Reciprocity Calibration," NRL Memorandum Report 3938 (1979).
25. L.P. Browder and S.W. Meeks, "Effects on One-Dimensional Stress on MIL-STD-1376 Piezoelectric Ceramic Materials, Types I, II, and III," NRL Report 8159 (Oct. 1977).
26. C.M. Thompson, NRL-USRD (private communication).
27. J.D. Plummer, Stanford University (private communication).

Appendix

LIST OF SAMPLES

Samples 1, 2, and 3 — Described in Fig. 2. Mentioned in section titled PIEZOELECTRIC CONSTANTS — ONE-DIMENSIONAL CONFIGURATION. Consist of a square piece of PVF₂ having an area of $\sim 1 \times 10^{-4} \text{ m}^2$ and cemented on both sides to stainless-steel plates. Used for measurements in one-dimensional configuration.

Samples a-2 and a-3 — Described in Fig. 9 configuration a. Mentioned in section titled PIEZOELECTRIC VOLTAGE COEFFICIENT FOR PVF₂ IN VARIOUS CONFIGURATIONS SUBJECTED TO HYDROSTATIC PRESSURE. They are actually samples 2 and 3 respectively, but with the alumina tube removed. Used for two-sided clamping tests.

Samples b-1 and b-2 — Described in Fig. 9 configuration b. Mentioned in section titled PIEZOELECTRIC VOLTAGE COEFFICIENT FOR PVF₂ IN VARIOUS CONFIGURATIONS SUBJECTED TO HYDROSTATIC PRESSURE. Consist of a circular piece of PVF₂ having an area of $3.88 \times 10^{-4} \text{ m}^2$ cemented on one side to a stainless-steel plate. Used for one-sided clamping tests.

Samples c-1 and c-2 — Described in Fig. 9 configuration c. Mentioned in section titled PIEZOELECTRIC VOLTAGE COEFFICIENT FOR PVF₂ IN VARIOUS CONFIGURATIONS SUBJECTED TO HYDROSTATIC PRESSURE. Consist of a square piece of PVF₂ having an area of $\sim 1.3 \times 10^{-4} \text{ m}^2$ cemented on one side to a stainless-steel plate. Used for one-sided clamping tests.

Samples d-1, d-2, and d-3 — Described in Fig. 9 configuration d. Mentioned in section titled PIEZOELECTRIC VOLTAGE COEFFICIENT FOR PVF₂ IN VARIOUS CONFIGURATIONS SUBJECTED TO HYDROSTATIC PRESSURE. Consist of a square piece of PVF₂ freely suspended. Used for hydrostatic tests.

Pre-POSFET Samples 5, 6, and 7 — Described in Figs. 13, 14, and 15, respectively. Mentioned in the section titled EVALUATION OF THE PRE-POSFET PIEZOELECTRIC TRANSDUCER. Consist of a square piece of PVF₂ cemented on one side to a sapphire substrate. Assembled at Stanford University and used for evaluating the pre-POSFET configuration.

Sample e — Described in Fig. 26 configuration e. Mentioned in the section titled HIGH AMPLITUDE DYNAMIC STRESS TRANSDUCER. Consists of a circular piece of PVF₂ having an area of $3.7 \times 10^{-5} \text{ m}^2$ cemented on one side to a brass plate. Used for dynamic pressure measurements.

Sample f — Described in Fig. 26 configuration f. Same as sample e except having an area of $3.85 \times 10^{-5} \text{ m}^2$.

Sample g — Described in Fig. 26 configuration g. Same as sample f except freely suspended.